Electronic Charge Transfer between Au Nano-Particles and TiO$_2$-terminated SrTiO$_3$(001) Substrate

K, Mitsuhara[1], Y. Kitsudo[1], H. Matsumoto[1], A. Visikovskiy[1], M. Takizawa[2], T. Nishimura[3], T. Akita[4], and Y. Kido[1]

Abstract

The interaction between Au nano-particles and oxide supports is recently discussed in terms of the catalytic activities.   This paper reports the electronic charge transfer between Au nano-particles and TiO$_2$-terminated SrTiO$_3$(001) substrate, which is compared with that for stoichiometric(S)-, pseudo-stoichiometric(S*)- and reduced(R)- TiO$_2$(110) supports. We observed the photoelectron spectra of Au 4f, O 2s, Ti 3p, and Sr 4p lines and also measured the work functions for Au/oxides supports using synchrotron-radiation light. As the results, all the O 2s, Ti 3p, and Sr 4p lines for Au/SrTiO$_3$(001) show lower binding energy shifts in a quite same manner and abrupt increase in the work function is seen in an initial stage. This clearly evidences an electronic charge transfer from the substrate to Au probably due to a much larger work function of Au than SrTiO$_3$(001), which leads to an upward band bending (0.3 eV) just like a Schottky contact. Electronic charge transfers also take place at Au/S- and Au/S*-TiO$_2$(110) and Au/R-TiO$_2$(110) interfaces, where electrons are transferred from Au to S- and S*-TiO$_2$ and from R-TiO$_2$ to Au, as predicted by *ab initio* calculations.

[1] *Department of Physics, Ritsumeikan University, Kusatsu, Shiga-ken 525-8577, Japan*

[2] *Rits SR Center, Ritsumeikan University, Kusatsu, Shiga-ken 525-8577, Japan*

[3] *Ion Beam Technology Center, Hosei University, Koganei, Tokyo 184-8584, Japan*

[4] *Advanced Industrial Science ad Technology, AIST Kansai, Ikeda, Osaka 563-8577, Japan*

1. Introduction

It is well known that Au is the noblest of all the metals. However, Haruta found that Au nano-particles dispersed on metal-oxide supports exhibit strong catalytic activities at a size about several nm[1-3]. So far, several models have been proposed to explain the emerging catalytic activities for Au/metal-oxide, in particular for Au/TiO$_2$(110). First principles calculations based on the density functional theory (DFT) predict importance of electronic charge transfer between Au nano-particles and supports[4-6]. For Au/MgO(001), Sanchez et al.[7] claimed that Au$_8$ clusters adsorbed to oxygen vacancies on the MgO surface are negatively charged and as a result weaken the molecular bond of O$_2$, leading to enhancement of oxidation of CO. In contrast, Wang and Hammer[6] demonstrated that Au$_7$ clusters adsorbed on an O-rich TiO$_2$(110) surface are cationic resulting in small activation barriers for the oxidation reaction of CO and O$_2$. Recently, observations by a scanning tunneling microscope (STM) showed that a water molecule adsorbs into O-vacancy and dissociates into OH and H on TiO$_2$(110)[8,9]. This hydroxyl (OH) may play some significant role in emerging catalytic activities in connection with Au nano-particles, just like a water-gas-shift catalysis[10]. In spite of many efforts, however, the mechanism leading to a strong catalytic activity of Au nano-particles is still a debatable issue.

In this study, we analyze the electronic properties of Au nano-particles deposited on TiO$_2$-terminated SrTiO$_3$(001) and stoichiometric(S)- and reduced(R)-TiO$_2$(110) substrates by photoelectron and photon-induced secondary electrons emission spectroscopy using synchrotron-radiation (SR) light. It is interesting to compare the interactions between Au nano-particles and the TiO$_2$ faces of oxide supports with different surface structures such as TiO$_2$-terminated SrTiO$_3$(001), S- and R-TiO$_2$(110) substrates. Indeed, SrTiO$_3$ and TiO$_2$ have similar band gaps of 3.2 eV (SrTiO$_3$) and 3.05 eV (TiO$_2$) and annealing in ultra high vacuum (UHV) creates vacancies of the oxygen on top, which form defect states in the band gap about 1 eV below the Fermi level. In the case of S-TiO$_2$(110), we prepared two types of surfaces by (i) annealing at 550˚C for 5 min in O$_2$ (1×10^{-6} Torr) and (ii) exposing the R-TiO$_2$(110) surface to O$_2$ at room temperature (RT). The different surface states are described in the next section. We first determine the areal occupation ratios of two (2D) and three dimensional (3D) Au islands formed on the above supports by medium energy ion scattering[11,12]. Here, the 2D island is defined as that with a height of one or two atomic layers. The shape of 3D islands is well approximated by a partial sphere with diameter d and height h[13]. The core level shifts of Au 4f, O 2s, Ti 3p and Sr 4p are observed by a hemispherical electrostatic analyzer, as a function of Au coverage. We also determine the work functions by measuring secondary electrons spectra from negatively biased Au/SrTiO$_3$(STO) and Au/TiO$_2$(110) samples, which are very sensitive to surface electronic states. All the above experiments were performed *in situ* under ultra-high vacuum (UHV) conditions ($\leq$ 2×10^{-10} Torr).

2. Experiment

The experiment was carried out at Beam-line 8 connected to a storage ring named AURORA working at Ritsumeikan SR Center. This beam-line consists of photoelectron spectroscopy (PES), high-resolution MEIS, and molecular beam epitaxy (MBE) systems[14,15]. Two types of varied-space-plane gratings cover photon energy from 20 up to 500 eV and incident photon energy was calibrated precisely by measuring Au 4 $f_{5/2,\,7/2}$ spectra for incidence of primary and the 2nd harmonic waves. A hemispherical electrostatic analyzer (ESA) detected emitted photoelectrons with an energy resolution better than 0.05 eV at a pass energy of 2.95 eV. The binding energy (E_B) of core levels was calibrated assuming the E_B value of 84.0 eV for Au $4f_{7/2}$ line emitted from bulk Au (In the previous analysis[11,12], we calibrated the E_B value by fitting the Fermi edge of Au 6s band). In the present MEIS analysis, we used 120 keV He^+ ions and scattered He^+ ions were energy-analyzed by a toroidal ESA with an excellent energy resolution ($\Delta E\,/\,E = 9 \times 10^{-4}$: FWHM), which makes it possible to determine the shape and size of Au nano-particles[13].

We prepared clean surfaces of Nb-doped (0.05 wt.%) n-type $SrTiO_3(001)$ substrates by sputtering with 1 keV Ar^+ followed by annealing at 550° C for 30 min in UHV. Annealing at 550° C for 30 min in O_2-pressure of 1×10^{-6} Torr led to a (1×1) surface without any contaminations (less than 1×10^{13} atoms/cm^2 for C). No O-vacancies and no surface segregation of Nb were confirmed by valence band spectra and by MEIS spectra, respectively. The structure of TiO_2-terminated $SrTiO_3(001)$ surface was reported previously[16]. The present MEIS analysis demonstrated the fraction of the TiO_2-face of more than 80 %. Similar sputtering/annealing treatment was also carried out for $TiO_2(110)$ and annealing at 800° C for 30 min in UHV changed the color from transparent to blue caused by introduction of O-vacancies in the bulk (F-center). Simultaneously, Ti interstitials are created, which act as an electron donor, resulting into an n-type semiconductor[17,18]. After observed a (1×1) pattern by reflection high-energy electron diffraction (RHEED), annealing at 550°C for 5min in O_2 ambient (1×10^{-6} Torr) led to the stoichiometric surface, S-$TiO_2(110)$. The R-$TiO_2(110)$ surface with bridging oxygen vacancies was obtained by annealing the S-$TiO_2(110)$ at 600°C for 5min in UHV, which was confirmed by detecting a Ti 3d defect state about 1 eV below the Fermi level. We also prepared the second type pseudo-stoichiometric $TiO_2(110)$ by exposing the R-$TiO_2(110)$ to O_2 at RT with an exposure of 5,000 L, which is, hereafter called S*-$TiO_2(110)$. According to the recent report by Wendt et al.[18], Ti interstitials are accumulated near the surface during annealing in UHV, which allow the adsorption of O_2 molecules onto 5-fold Ti atoms. In this respect, the S*-$TiO_2(110)$ surface has no bridging O (O_{br})-vacancies but has the O adatoms (O_{ad}) on the 5-fold Ti. In fact, the S- and S*-$TiO_2(110)$ surfaces have different work functions, as presented later.

Au was then deposited on the clean surfaces at RT with a Knudsen cell at a rate of 0.30 ML/min under UHV condition. Here, 1 ML means 1.39×10^{15} atoms/cm^2, corresponding to the areal density

of Au(111).　The shape and average size of Au nano-particles together with the absolute amount of Au (areal occupation ratios of 2D and 3D islands) were determined by high-resolution MEIS[13].

3. Results and Discussion

3-1. Growth Mode

We previously reported the growth modes and electronic properties of Au nano-particles deposited on S- and R-TiO$_2$(110) and NiO(001) substrates[11,12].　For S-TiO$_2$(110) and NiO(001), 2D-islands grow initially and then 3D-islands growth becomes dominant.　Here, an island with a height of one or two atomic layers is defined as a 2D-island and as mentioned before, the shape of 3D islands is well approximated by a partial sphere with diameter d and height h[13].　In the case of R-TiO$_2$(110), the bridging O-vacancies act as an anchor for nucleation and thus 3D-islands start to grow at a very early stage.　In contrast to Au growth on TiO$_2$, there are few reports on Au deposited onto STO(001)[19,20].
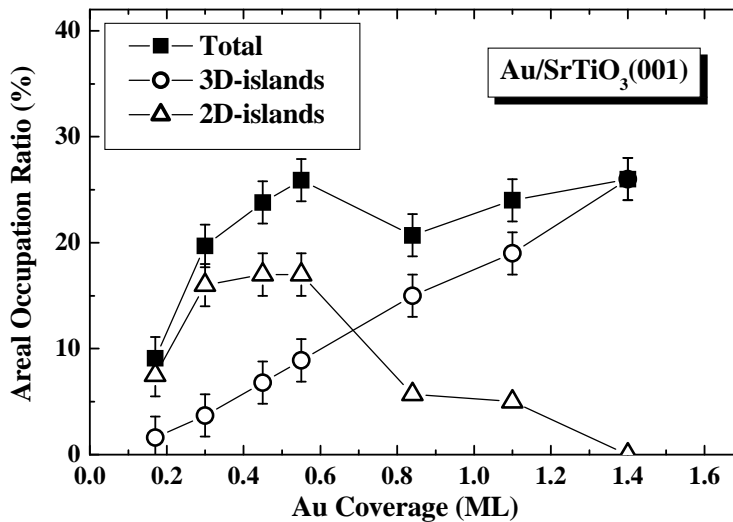
FIG. 1.　Areal occupation ratios of 2D (σ_{2D}: triangles) and 3D (σ_{3D}: open circles) islands grown on SrTiO$_3$(001) as a function of Au coverage.　Here, 2D islands are defined as those with a height of one ($\underline{1} \times 1.39 \times 10^{15}$ atoms/cm^2) or two atomic layers.　Squares denote total occupation ratios (σ).

Figure 1 shows the areal occupation ratios (σ_{2D}, σ_{3D}) of 2D- and 3D-islands of Au nano-particles grown on STO(001), which were determined by MEIS, as a function of Au coverage. Obviously, 2D-islands grow initially up to Au coverage of 0.6 ML and then 3D-islands growth becomes dominant.　Such a growth mode is quite similar to that for Au/S-TiO$_2$(110) and different from the Au/R-TiO$_2$(110) case[11,12].　Shown in Fig. 2 are the diameter and height of 3D-islands as a function of Au coverage for Au/STO(001).　The diameter d takes a constant value of 2.2 nm up to Au coverage of 0.6 ML and then increases almost linearly with increasing Au coverage, while the

height increases gradually with Au coverage.   There is a competition between surface and interface energies to lower the total energy of an Au particle.   Presence of a critical lateral size suggest that above such a critical value, growth of a 3D island with a shape of partial sphere is energetically favorable rather than keeping a 2D island in order to reduce the total energy.   Such a critical diameter for transition from 2D to 3D islands is also seen for S-TiO$_2$(110) substrates (~ 2 nm) but not for R-TiO$_2$(110) for Au coverage above 0.1 ML due to presence of the bridging O-vacancies on the surface acting as a nucleation site.   The lateral size and areal occupation ratio (σ_{3D}) of 3D islands determined by MEIS are consistent with the image observed by a scanning electron microscope of a field emission type (FE-SEM) (not shown here).   Note that such 2D islands cannot be viewed by FE-SEM and transmission electron microscopes.
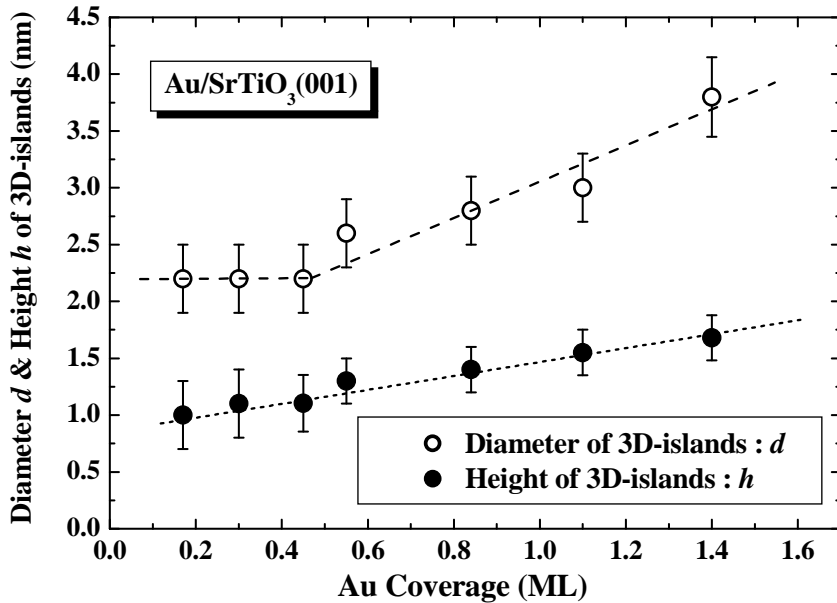
FIG. 2.   Diameter d (open circles) and height h (full circles) of Au 3D-islands grown on SrTiO$_3$(001) as a function of Au coverage.

3-2. Core level Shifts

Our primary concern is concentrated on the electronic properties of Au nano-particles on oxide supports.   Figure 3 shows the Au 4f$_{5/2,7/2}$ lines observed at a photon energy of 140 eV for Au/STO(001) by varying Au coverage.   As clearly seen, the Au 4f line shifts toward the higher E_B side with decreasing Au coverage, which were also observed for Au/S-TiO$_2$(110), Au/S*-TiO$_2$(110) and Au/R-TiO$_2$(110) (see Fig. 4).   Electronic charge transfer between Au and support is sometimes discussed in terms of the binding energy (E_B) shift of Au 4f line observed by photoelectron spectroscopy[21-23].   However, in the previous study[24], we showed that higher E_B shifts of Au 4f line are well scaled by the number of Au atoms per particle and independent of the support species

and thus originated from the effect of a photo-hole remaining on a metal nano-cluster immediately after a photoelectron emission, so called final state effect[25-27]. This attractive interaction between the hole and emitted electron gives an apparent higher binding energy shift. The final state effect is diminished with increasing the Au particle size, because a larger amount of residual conduction electrons respond to cancel the electric field of the hole. There are some efforts to distinguish the initial (charge transfer) and final state effects by Auger electrons and characteristic X-ray spectra[26,28]. However, the treatment is based on the assumption that the relevant three electronic states undergo equal E_B shifts and identical relaxation schemes, which are still ambiguous. Therefore, it is essential to observe the core level shifts of the composite elements of supports as well as work functions to judge an electronic charge transfer from Au to support or vice versa.
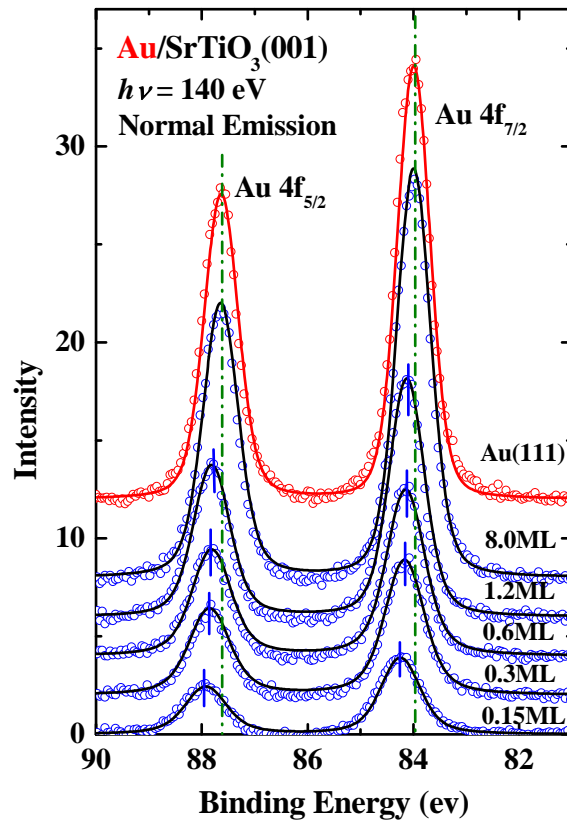
FIG. 3. Au 4f core level spectra observed for Au/STO(001) at photon energy of 140 eV as a function of Au coverage. Solid curves correspond to best-fit spectra using Voigt function.

Shown in Fig. 5(a) is the core level spectrum of O 2s and Sr $4p_{1/2,3/2}$ observed at a photon energy of 140 eV for Au(0.15 ML)/STO(001). The spectrum is well decomposed into three components, O 2s (E_B: 22.56 eV) and Sr 4p ($4p_{1/2}$: 20.46 eV, $4p_{3/2}$: 19.26 eV) using Voigt functions and assuming the branching ratio of 2.0 for Sr $4p_{1/2,3/2}$. The O 2s and Sr $4p_{1/2,3/2}$ spectra observed for varied Au coverage are shown in Fig. 5(b). It is clearly seen that the E_B values of both O 2s and Sr 4p lines shift toward a lower energy side with increasing Au coverage. Interestingly, as indicated in Fig. 6,

the O 2s, Sr $4p_{3/2}$ and Ti 3p lines shift toward a lower energy side in a quite same manner with increasing Au coverage and the E_B shifts are saturated at −0.3 eV. Here, we should note that the escape depth of photo-electrons is estimated to be ~0.6 nm[29] and the areal occupation ratio of Au particles is estimated to be about 45 % from MEIS analysis for Au coverage of 5 ML. The above E_B shifts clearly evidence an upward band bending of 0.3 eV, indicating an electronic charge transfer from $SrTiO_3$(001) support to Au nano-particles. This suggests that electrons transferred into Au nano-particles are located at the interface and resultant electron deficiencies (holes) are diffused toward the inside to some extent to equalize the Fermi levels, just like formation of a Schottky contact. Indeed, the work function of Au (5.36 eV) is considerably larger than that of $SrTiO_3$(001) (3.6±0.1 eV), which is shown later. If one assumes a diffusion length of 10 nm and the number of diffused electron deficiencies of ~10^{14}/cm^2, one obtains an upward band bending of 0.3 eV employing the dielectric permittivity of $300\varepsilon_0$ for STO (ε_0 : dielectric constant of vacuum).
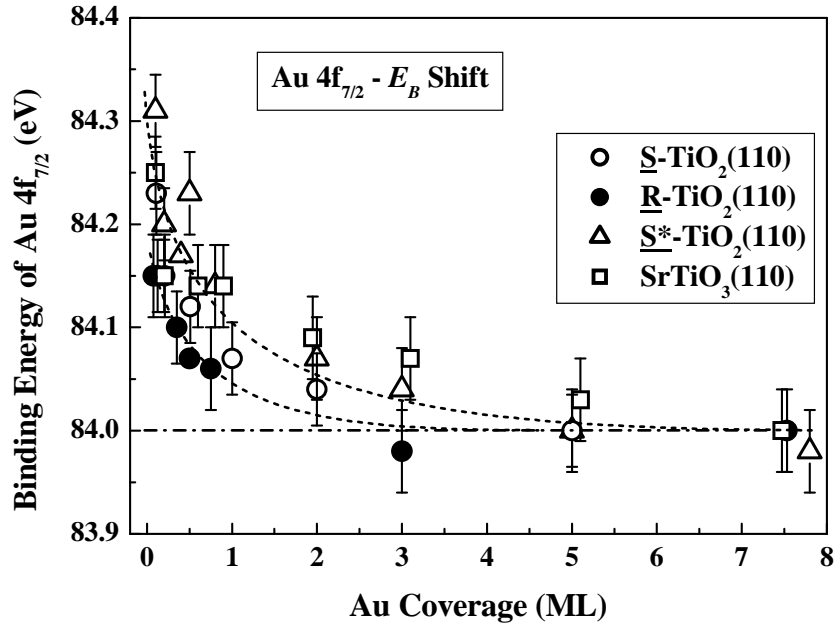
FIG. 4. Binding energy of Au $4f_{7/2}$ observed for $SrTiO_3$(001) (squares), S-TiO_2(110) (open circles), S*-TiO_2(110) (triangles) and R-TiO_2(110) (full circles) substrates as a function of Au coverage. Dotted curves are drawn to guide the eyes.

For the S-, S*- and R-TiO_2(110) supports, we also find electronic charge transfers between Au and the support. Shown in Fig. 7 are the E_B shifts of O 2s and Ti 3p lines for S- and S*-TiO_2(110) (upper) and R-TiO_2(110) (lower) substrates, as a function of Au coverage. In the case of S- and S*-TiO_2(110), lower E_B shifts take place for both O 2s and Ti 3p lines even though very small and the E_B shifts of O 2s are significantly larger than those of Ti 3p, indicating that the valence electrons

of Au tend to be attracted to underlying O atoms rather than Ti atoms. However, the interaction between Au and the support is very weak because of small E_B shifts (≤ 0.2 eV) of O 2s and Ti 3p. The electronic charge transfer presented here means a polarization of the spatial distribution of valence electrons, which leads to formation of local electric dipoles at the Au/support interfaces not an upward band bending because of the O 2s and Ti 3p E_B shifts in a different manner (see Fig. 7).
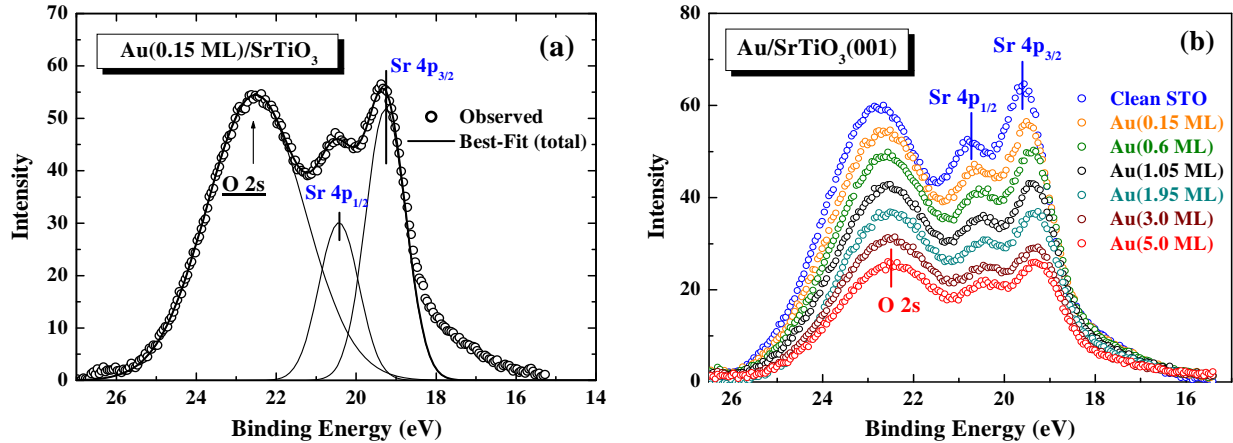
FIG. 5. (a) Core level spectra of O 2s and Sr $4p_{1/2,3/2}$ observed at a photon energy of 140 eV for Au(0.15 ML)/STO under normal emission condition. The spectrum is deconvoluted into three components, O 2s (E_B: 22.56 eV) and Sr 4p ($4p_{1/2}$: 20.46 eV, $4p_{3/2}$: 19.26 eV) using Voigt functions. (b) O 2s and Sr $4p_{1/2,3/2}$ spectra as a function of Au coverage.

In contrast, for the R-TiO$_2$(110) support, slightly lower E_B shifts are also seen for both Ti 3p and O 2s lines, suggesting an electronic charge transfer from Au to the support. However, as discussed later, this apparent lower E_B shifts come from relaxation of an initial downward band bending, which is estimated to be ~0.2 eV from lower E_B shifts of O 2p bonding/nonbonding states by exposure to O$_2$ at RT[12,30]. Recent resonant photoelectron diffraction analysis showed that the defect charge is distributed over several surface and subsurface lattice Ti sites[31]. The E_B values of the O 2p bonding/nonbonding states are shifted to lower binding energy side by Au deposition[12,32], correlating with the Ti 3p and O 2s lines. Based on the *ab initio* calculations, Okazaki et al.[5] predicted that the hybridization at the Au/S-TiO$_2$(110) interface is weak, while an electronic charge transfer (a polarization of the spatial distribution of valence electrons) from TiO$_2$ to Au takes place at Au/R-TiO$_2$(110). This is supported by other theoretical predictions based on the first principles calculations[6,8]. In this case, electron deficiencies (holes) created in the support probably diffuse inside and recombine with the initially distributed electrons of the R-TiO$_2$. Indeed, the electronic charge transfer from the substrate to Au is indicated by the observed work functions, as presented later.
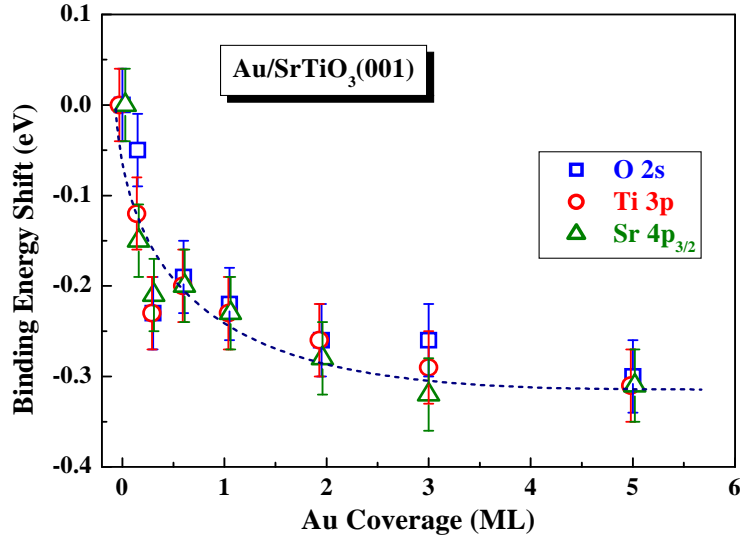
FIG. 6.   Binding energy shifts of O 2s (squares), Ti 3p (circles) and Sr 4p$_{3/2}$ (triangles) observed for Au/SrTiO$_3$(001) as a function of Au coverage.   Curve is drawn to guide the eyes.
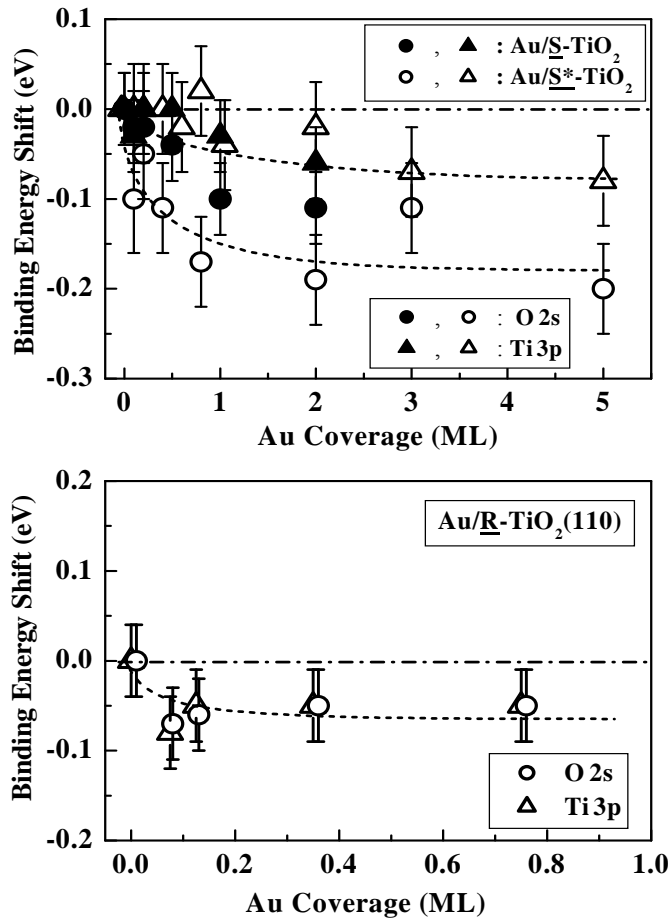
FIG. 7.   Binding energy shifts of O 2s (circles) and Ti 3p (triangles) observed for Au on S- and S*-TiO$_2$(110) (top) and for Au/R-TiO$_2$(110) (bottom) as a function of Au coverage.

3-3. Work Functions

The electric dipole induced by an electron charge transfer at an Au/support interface should change the work function (Φ) at a relatively low Au coverage.　Figure 8 shows the secondary electrons spectra measured for clean STO(001) and Au/STO(001) at Au coverage of 0.1, 0.2 and 0.4 ML.　Here, SR-photons were incident at 140 eV on the samples which were negatively biased (V_B = −7.6 V).　By measuring the on set of the kinetic energy of secondary electrons E_{kin}, we can deduce the work function Φ experimentally.

$$\Phi = \Phi_{SP} + E_{kin} + e\,V_B, \tag{1}$$

where e is electron charge (-1.6×10^{-19} C) and Φ_{SP} the work function of the spectrometer employed (known).　The work functions determined here are indicated in Fig. 9, as a function of Au coverage. The Φ value increases drastically at low Au coverage and then gradually approaches that of bulk Au (5.36 eV).　This drastic increase in work function is intimately related to the upward band bending caused by a dipole formed at the Au/STO(001) interface (Au: negative & STO: positive),
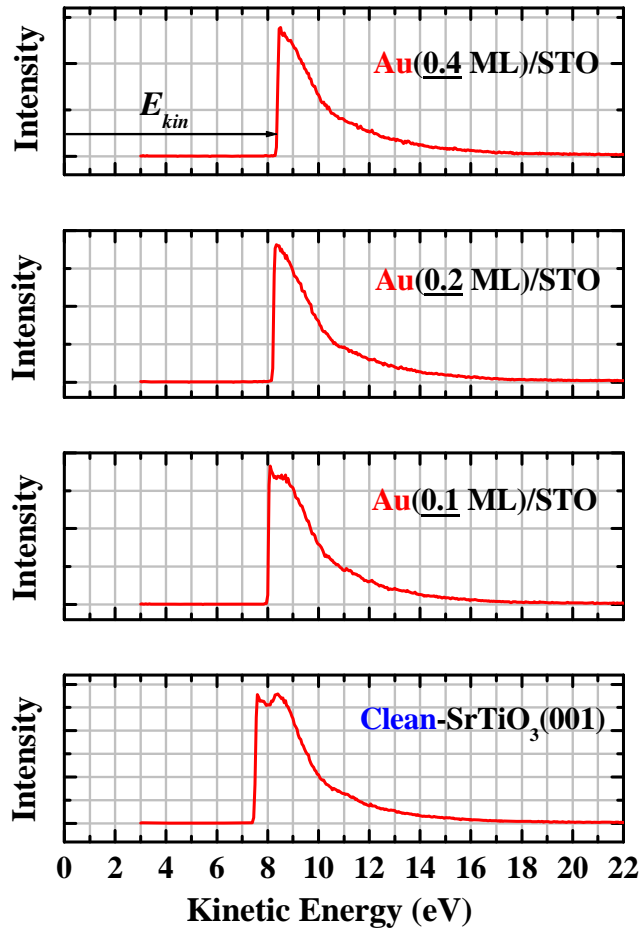
FIG. 8.　Secondary electrons spectra measured at photon energy of 140 eV.　From the bottom to the top, clean SrTiO₃(001), Au(0.1 ML)/STO, Au(0.2 ML)/STO and Au(0.4 ML)/STO.　Samples were negatively biased at −7.6 V against the ground.

latter (ii) undergoes more effectively the electric filed of the interface dipoles near the perimeter of Au particles.   The third is the component from Au nano-particles, which is insensitive to the interface dipoles because of screening of the conduction electrons of overlying Au particles that respond to delete the electric field of the interior interface dipoles.   In general, the secondary electrons intensity from semiconductors and insulators is considerably larger than that from metals. In spite of negatively charged Au at the Au/STO interface, the Au 4f line shifts toward the higher E_B side, which is ascribed to the final state effect.   The fractional intensity is small enough for the photoelectrons from the Au 4f state emitted near the periphery of Au nano-particles, which undergo the electric field of the interface dipoles.   Further increase in Au coverage leads to gradual increase in work function, which finally reaches the work function of Au.
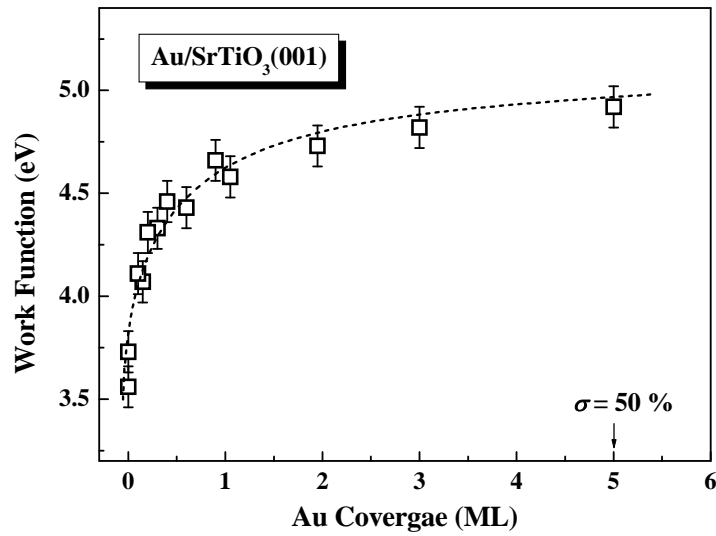
FIG. 9.   Work functions measured from secondary electrons emission spectra for Au/STO(001) as a function of Au coverage.   Dotted curve is drawn to guide the eyes.

It is intriguing to compare the work functions of Au/STO(001) with those of Au/S-TiO$_2$(110), Au/S*-TiO$_2$(110) and Au/R-TiO$_2$(110).   Figure 10 depicts the work functions measured for Au/S-TiO$_2$(110) (open circles and squares), Au/S*-TiO$_2$(110) (open triangles) and Au/R-TiO$_2$(110) (closed symbols) with different O-vacancy concentration in the bulk TiO$_2$.   It is found that higher defect concentration gives a higher Φ value and the work function for S-TiO$_2$(110) is $0.3 - 0.4$ eV larger than that for R-TiO$_2$(110).   The work functions of TiO$_2$(110) surfaces scatter largely owing to strong dependence upon bulk and surface defect densities.   Note that work function consists of bulk (Φ_B) and surface dipole (Φ_S) terms[33,34].   The latter term comes from the fact that electrons avoid each other due to repulsive Coulomb interactions, as a result an electron gains a negative potential energy called exchange-correlation potential.   The work functions of S-, S*- and R-TiO$_2$(110) surfaces depends on the density of the surface and bulk O-vacancies as well as Ti interstitials near the surface[18].   Indeed, the work functions observed for S-, S*- and R-TiO$_2$(110)

surfaces with almost a same bulk defect density(same substrate) are 5.12 ± 0.05, 4.91 ± 0.05 and 4.79 ±0.05 eV, respectively.   The surface term originates from a surface dipole consisting of positive cores and valence electrons near a surface, which is, of course, dependent upon surface structures. As shown in Fig. 10, a small Au coverage less than 0.5 ML on S- and S*-TiO$_2$(110) leads to abrupt reduction of work function, which is correlated with the electronic charge transfer from Au to S-TiO$_2$(110) support, as mentioned before (see Fig. 7).   With further increasing Au coverage, the work function gradually increases and approaches that of the bulk Au (5.36 eV).   In contrast, a small amount of Au deposition on R-TiO$_2$(110) increases the work function steeply and then gradually approaches that of the bulk Au.   This is ascribed to the electronic charge transfer from R-TiO$_2$(110) substrate to Au, as predicted by the *ab initio* calculations[5,6].   Indeed, the slightly lower E_B shifts of Ti 3p and O 2s (see Fig. 7) are probably due to relaxation of the downward band bending as the result of the above electronic charge transfer.   Despite the negatively charged Au at the Au/R-TiO$_2$ interface, higher E_B shifts for the Au 4f line are observed (see Fig. 4), which is also caused by the final state effect.   Here, we emphasize that the variation of the work functions before and after a small amount of Au deposition gives more reliable information about the electronic states of near surface regions rather than the core level shifts of Au and constituents of the supports which are affected by the final state effect and band bending.
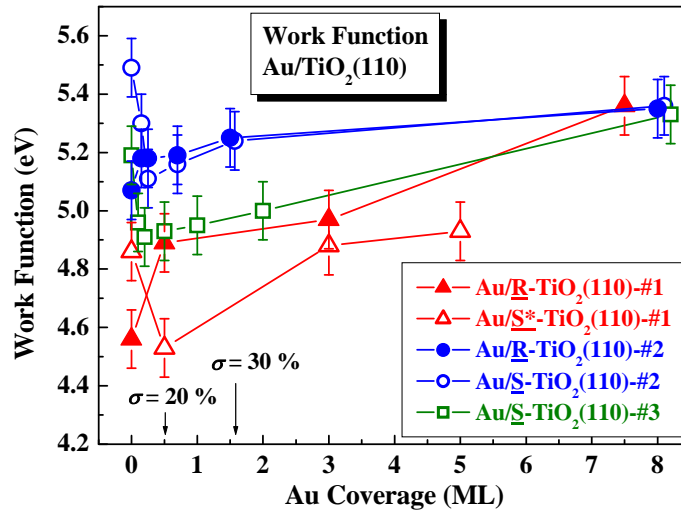
FIG. 10.   Work functions measured for Au/S-TiO$_2$(110) (open circles and squares), Au/S*-TiO$_2$(110) (open triangles) and Au/R-TiO$_2$(110) (full symbols) as a function of Au coverage. Circles (#1), squares (#2), and triangles (#3) correspond to samples with high, medium, and low concentrations of bulk O-vacancies, respectively and σ is total areal occupation ratio ($\sigma_{2D} + \sigma_{3D}$) of Au nano-particles.

As described above, the present results demonstrate that there are significant interactions

between Au nano-particles and oxide-supports, which lead to electronic charge transfers at the interfaces.   The interactions are quite sensitive to the structures of the oxide surfaces including the presence/absence of O-vacancies even though they have same TiO_2 faces.   From the work functions and the core level shifts of the composite elements of the oxide supports, an electronic charge transfer takes place (i) from STO to Au resulting in an upward band bending of 0.3 eV just like a Schtottky contact.   This is ascribed to much lager work function of Au (5.36 eV) than that of STO(3.6 eV), which promotes electrons transfer from STO to Au in spite of a weak interaction between Au and TiO_2[20], although the atomistic and electronic mechanism is not clear at the present. In the case of Au/S*-TiO_2(110), a local small dipole is induced due to an electronic charge transfer from Au to the underlying O atoms, whereas an electronic charge transfer from R-TiO_2(110) to Au occurs, as predicted by DFT calculations[5,6], leading to relaxation of the down ward band bending. At the present, however, such different interactions at the Au/oxide-supports cannot be explained quantitatively.   It is indispensable to compare the present analysis with the *ab initio* calculations which can give an insight into the interaction between Au nano-particles and the oxide support with different structures of TiO_2 faces.   In the *ab initio* calculations, however, the number of Au atoms of the clusters is limited to a small amount and the information about kinetic behaviors such as diffusion of electrons (holes) is also insufficient.

4. Summary

The electronic properties of Au nano-particles grown on TiO_2-terminated STO(001) (≥ 80 %) and S-, S*- and R-TiO_2(110) substrates were analyzed by photoelectron and secondary electrons spectroscopy using SR-light.   Simultaneously, the shape and size as well as the areal occupation ratios of Au nano-particles are also determined by high-resolution MEIS.   The growth mode of Au on TiO_2-terminated STO(001) is basically similar to that on S- and R-TiO_2(110).   We observed the core level shifts of Au 4f, Ti 3p, Sr 4p and O 2s lines together with the work functions, which were derived from the spectra of secondary electrons emitted by photon irradiation.   As a result, it is found that a significant electron charge transfer takes place at Au/STO(001) interface from STO support to Au nano-particles due to a much larger work function of Au than that of STO(001).   The electron deficiencies created near the STO surface diffuse toward the inside and thus lead to an upward band bending of 0.3 eV, just like a Schottky contact.   In the case of S-, and S*-TiO_2(110) supports, an electronic charge transfer occurs from Au to underlying O rather than Ti of the support even though very small, which forms a local interface dipole and does not induce a band bending. In contrast, for Au/R-TiO_2(110) an electronic charge transfer takes place from the support to Au, which is evidenced by the abrupt increase in the work function in the initial stage of Au deposition. The results obtained for Au on S- and R-TIO_2(110) are consistent with the theoretical predictions based on the first principles calculations, although the hybridization for Au/S-TiO_2(110) is predicted

to be very weak.

Acknowledgment

References

[1] M. Haruta, T. Kobayashi, H. Sano, and N. Yamada, Chem. Lett. **2** (1987) 405.

[2] M. Haruta, Catal. Today **36**, 153 (1997).

[3] M. Valden, X. Lai, and D.W. Goodman, Science **281** (1998) 1647.

[4] L.M. Molina and B. Hammer, Phys. Rev. **B 69** (2004) 155424.

[5] K. Okazaki, Y. Morikawa, S. Tanaka, K. Tanaka, and M. Kohyama, Phys. Rev. **B 69** (2004) 235404.

[6] J.G. Wang and B. Hammer, Phys. Rev. Lett. **97** (2006) 136107.

[7] A. Sanchez, S. Abbet, U. Heiz, W.D. Schneider, H. Häkkinen, R.N. Barnett, and U. Landman, J. Phys. Chem. **A 103** (1999) 9573.

[8] S. Wendt, J. Matthiesen, R. Schaub, E.K. Vestergaard, E. Lægsgaard, F. Besenbacher and B. Hammer, Phys. Rev. Lett. **96** (2006) 066107.

[9] T. Minato, Y. Saino, Y. Kim, H.S. Kato, K. Aika, M. Kawai, J. Zhao, H. Petek, T. Huang, W. He, B. Wang, Z. Wang, Y. Zhao, J. Yang and J.G. Hou, J. Chem Phys. **130** (2009) 124502.

[10] Z-P. Liu, S.J. Jenkins, and D.A. King, Phys. Rev. Lett. **94** (2005) 196102.

[11] T. Okazawa, M. Fujiwara, T. Nishimura, T. Akita, M. Kohyama and Y. Kido, Surf. Sci. **600** (2006) 1331.

[12] T. Okazawa, M. Kohyama, and Y. Kido, Surf. Sci. **600** (2006) 4430.

[13] A. Iwamoto, T. Okazawa, T. Akita, I. Vickridge and Y. Kido, Nucl. Instrum. Methods **B266** (2008) 965.

[14] Y. Kido, H. Namba, T. Nishimura, A. Ikeda, Y. Yan and A. Yagishita, Nucl. Instrum. Methods **B 136-138** (1998) 798.

[15] T. Nishimura, A. Ikeda, and Y. Kido, Rev. Sci. Instrum. **69** (1998) 1671.

[16] T. Nishimura, A. Ikeda, H. Namba, T. Morishita and Y. Kido, Surf. Sci. **421** (1999) 273.

[17] M. Aono and R.R. Hasiguti, Phys. Rev. **B 48** (1993) 12406.

[18] S. Wendt, P.T. Sprunger, E. Lira, G.K.H. Madsen, Z. Li, J.Ø. Hansen, J. Matthiesen, A. B.-Rasmussen, E. Lægsgaard, B. Hammer and F. Besenbacher, Sci. **320** (2008) 1755.

[19] F. Silly and M.R. Castell, Phys. Rev. Lett. **96** (2006) 086104.

[20] J. Wang, X.S. Wu, J. Zhou and J.M. Dong, Chem, Phys. **360** (2009) 79.

[21] H.-G. Boyen, G. Kästle, F. Weigl, P. Ziemann, G. Schmid, M.G. Garnier, and P. Oelhafen, Phys. Rev. Lett. **87** (2001) 276401.

[22] Z. Zhao, T. Diemant, D. Rosenthal, K. Christmann, J. Bansmann, H. Rauscher, and R.J. Behm, Surf. Sci. **600** (2006) 4992.

[23] M.S. Chen, D.W. Goodman, Catal. Today **111** (2006) 22.

[24] Y. Kitsudo, A. Iwamoto, H. Matsumoto, K. Mitsuhara, T. Nishimura, M. Takizawa, T. Akita, Y.

Maeda, and Y. Kido,　Surf. Sci. **603** (2009) 2108.

[25] G.K. Wertheim, S.B. DiCenzo and S.E. Youngquist,　Phys. Rev. Lett. **51** (1983) 2310.

[26] G.G. Kleiman, R. Landers, P.A.P. Nascente, and S.G.C. de Castro,　Phys. Rev. **B 46** (1992) 4405.

[27] H. Hövel, B. Grimm, M. Pollmann and B. Reihl,　Phys. Rev. Lett. **81** (1998) 4608.

[28] K. Luo, X. Lai, C.-W. Yi, K.A. Davis, K.K. Gath, and D.W. Goodman,　J. Phys. Chem. **B 109** (2005) 4064.

[29] S. Tanuma, T. Shiratori, T. Kimura, K. Goto, S. Ichimura, and C.J. Powell,　Surf. Interface Anal. **37** (2005) 833.

[30] U. Diebold,　Surf. Sci. Reports **48** (2003) 53.

[31] P. Krüger, S. Bourgeois, B. Domenichini, H. Magnan, D. Chandesris, P.Le Fèvre, A.M. Flank, J. Jupille, L. Floreano, A. Cossaro, A. Verdini and A. Morgante,　Phys. Rev. Lett. **100** (2008) 055501.

[32] T. Minato, T. Susaki, S. Shiraki, H.S. Kato, M. Kawai, and K. Aika,　Surf. Sci. **566-568** (2004) 1012.

[33] A. Zangwill,　*Physics at Surfaces* (Cambridge University Press, Cambridge, 1988).

[34] M.C. Payne, M.P. Teter, D.C. Allan, T.A. Arias and J.D. Joannopoulos,　Rev. Mod. Phys. **64** (1992) 1045.